RADIAL VIBRATION ANALYSIS OF A VERTICAL ROTOR WITH A TILTING-PAD THRUST BEARING

André Garcia Chiarello
Universidade Federal de Itajubá, Departamento de Mecânica, CP 50, CEP 37500.903, Itajubá, MG, Brasil, e-mail: andre@iem.efei.br.

Vimar Arthur Schwarz
Universidade Federal de Itajubá, Departamento de Mecânica, CP 50, CEP 37500.903, Itajubá, MG, Brasil, e-mail: vilmar@iem.efei.br.

Abstract. Traditional methods for monitoring practical rotating machinery are usually based on Fourier transforms, such as, spectral analysis, cepstrum and time-frequency analysis. It is well known that some machine faults produce representative spectral lines and one can try to associate these spectral lines to the faults. However, machine faults may have virtually the same spectral representation and hence, one can find difficulties to distinguish one fault from another. Recently, evidences of nonlinear behavior have been reported in rotor systems with rub or clearance, which suggest the use of nonlinear methods for condition monitoring and fault detection. In this paper the pseudo-phase portrait (PPP) is used for condition monitoring of a practical rotating machine. The PPP is based on eigenvalue-eigenvector decomposition of the reconstructed phase-state. The diagrams visualized in PPP preserve the most important characteristics of the trajectory, and also have advantages over conventional methods, such as its robustness to signal noise and its sensibility to small variations of machine conditions. The PPP analysis obtained under different machine conditions demonstrates that it is possible to detect major differences in system dynamics. A vertical machine with a tilting pad thrust bearing was used to investigate the PPP method and the preliminary results showed that the method is appropriate for detecting small variations in bearing loads and also it is capable of detecting bearing faults. It is promising, therefore, that PPP can be successfully used for fault detection in rotating machinery.

Key words. Pseudo-phase portrait, machine monitoring, fault diagnosis.

1. Introduction

The rotating machinery used for electric generation such as hydraulic generator or gas turbines have fundamental importance, not only for industrial use, but also for improving the quality of life in any community. In this context, the machine condition monitoring is an indispensable task for lowering the maintenance costs and also for avoiding any undesirable interruption in energy supply. Most methods for practical machinery monitoring are based on Fourier transforms or fast Fourier transforms (FFT), such as spectral analysis, cepstrum and time-frequency analysis. The common approach for practical applications is to use vibration sensors, such as accelerometers, which are positioned on the bearings and on-line data acquisition software is used for monitoring the machine operational conditions. The main drawback in this conventional approach is the fact that an incipient fault usually has negligible spectral representation and this can be interpreted as signal noise or regular variations of machine conditions. Also, different rotating machine faults may have virtually the same spectral representation, and this complicates the task of fault diagnosis.

To overcome the limitations of these conventional techniques, new monitoring methods have been proposed for practical applications in large rotating machinery (Lucifredi et al., 2000; Chen, 1995). The most desired characteristics of these new methods are: sensibility to small variations of machine conditions, the capacity of distinguishing different faults and robustness to signal noise. The conventional methods are based on machine symptoms and therefore, initially the fault patterns have to be developed and stored in the computer. Then they are compared to the current pattern and some classification method indicates the presence of anomalies. The extraction of fault features and diagnostic indices are particularly important in these methods once few analytical models can satisfactorily describe the behavior of a large rotating machine.

The orbit portrait analysis is another usual method for monitoring rotating machinery. Unlike spectral analysis, which is a frequency domain technique, orbit portrait is a time domain technique, which uses the raw time series of the shaft displacements. The usual approach for practical computation of orbit diagrams is to use at least two non-contact displacement sensors, fixed to the bearing cases in orthogonal axis. The relative shaft motions between bearing case and the shaft are measured and plotted in a X-Y co-ordinate plane. The trajectory of the center of the shaft can be observed and monitored in on-line equipments. If a fault appears, it is expected some modifications in the orbit diagram and after that, some diagnostic routine is employed. The orbit analysis is an effective technique for bearing monitoring, however it is difficult to distinguish small machine variations in such type of diagrams. For example, a small rotation variation produces usually negligible orbit variation, once the velocity is not used in orbit calculations and this could be a serious problem in electrical generators.

Recent researches have shown that some rotating machine faults introduce complicated nonlinear vibration characteristics. Chaotic motions can be found in large rotating machine with unstable oil film, cracked rotor, rotor-to-

stator rub or a loose pedestal (Muszinska, 1995; Chu, 1997; Muller, 1994). Hence it is necessary to develop nonlinear methods for effective machine monitoring and fault diagnosis. The conventional approaches for nonlinear system analysis are based on phase portrait, Poincaré maps and bifurcation diagrams. The phase portrait is an orthogonal vector plot of the displacement vector $x(t)$ and its temporal derivative $\dot{x}(t)$. The periodicity of an ideal linear system can be easily visualized because the attractors of the trajectory are stable. For a nonlinear motion the attractors become more complex and the analysis of this trajectory is not so obvious.

In real word, the machine signals are not ideal, because they are inevitably associated with noise. This fact introduces an additional problem in the phase portrait analysis, because one has to calculate the derivatives of raw time series. The development of nonlinear dynamic has brought new methodologies to investigate complex behavior of rotating machinery. Wang (2001) compared three different nonlinear methodologies for fault diagnosis in rotating machinery, which are: pseudo-phase portrait, singular spectrum analysis and correlation dimension. The correlation dimension of a non-linear dynamical system gives an indication of the number of degrees of freedom excited in the system. A fault introduces a modification in system behavior and some variation of correlation dimension is expected (Jiang, 1999). The singular spectrum analysis indicates the complexity of the signal. A pair of eigenvalues in the singular spectrum corresponds to a line in the conventional spectrum. So, the larger the effective dimension of the subspace in a singular spectrum, more complex the signal will be (Wang, 2000).

The pseudo-phase portrait is simple to compute and seems to be sensitive to some fault types. Some interesting pseudo-phase portraits from a large rotating machine with oil whirl fault and rotor-to-stator rub fault have been reported by Wang (2003). By comparing with the phase portrait, the major features of the pseudo-phase portrait theory seem to be its robustness to noise and the preservation of geometrical invariants, such as, the fractal dimension of an attractor and the Lyapunov exponents of a trajectory. In this work, the pseudo-phase portrait technique was applied to a vertical test machine with a tilting pad thrust bearing for condition monitoring. The basic theory of pseudo-phase portrait is stated and discussed in Section 2.

2. Pseudo-phase portrait

The pseudo-phase portrait is an application of the method of delays that was originally proposed by Takens (1981) and adapted for practical machine diagnosis by Wang (2003). The main idea of the method of delays is that it is unnecessary to know the signal derivatives to form a co-ordinate system in which the phase-portrait diagrams are plotted. This approach uses directly the raw time series and its lagged values to construct the state space, avoiding the use of derivatives. For a *N*-point time series $\{x_1, x_2, \cdots, x_N\}$ a sequence of vectors $\boldsymbol{y}_i$, $i = 1, 2, \cdots, M$, can be generated to form a trajectory matrix $\boldsymbol{A}$ in the form:

$$\boldsymbol{A} = \begin{bmatrix} \boldsymbol{y}_1^T \\ \boldsymbol{y}_2^T \\ \vdots \\ \boldsymbol{y}_M^T \end{bmatrix} = \begin{bmatrix} x_1 & x_{1+\tau} & \cdots & x_{1+(m-1)\tau} \\ x_2 & x_{2+\tau} & \cdots & x_{2+(m-1)\tau} \\ \vdots & \vdots & \vdots & \vdots \\ x_M & x_{M+\tau} & \cdots & x_{M+(m-1)\tau} \end{bmatrix} \tag{1}$$

where $M = N - (m-1)\tau$ is the length of the reconstructed vectors $\boldsymbol{y}_i$. Each vector $\boldsymbol{y}_i$ has the dimension *m* and corresponds to the reconstructed state-space vector. The dimension *m* is called embedding dimension of the reconstructed state space, τ is the lag time measured in units of sampling interval. The space, which is reconstructed from raw time series, is called the embedding space or pseudo-phase space and the trajectory in the pseudo-phase space is called pseudo-phase portrait (PPP).

The problem of plotting the trajectory matrix in this form is the presence of redundant vectors, which add little information about the system. Hence, it is convenient to introduce some linear transformation of trajectory matrix to achieve a sequence of linearly independent vectors. In particular, one can calculate the number of linearly independent vectors that can be constructed from the trajectory matrix. Mathematically, one can define the singular vectors $\boldsymbol{s}_i$, which satisfy the condition:

$$\boldsymbol{s}_i^T \boldsymbol{A} = \sigma_i \boldsymbol{c}_i^T \tag{2}$$

where, σ_i, $i = 1, 2, \cdots, m$, are real numbers and the linearly independent vectors $\boldsymbol{c}_i$ form the desired orthogonal base. Broonhead (1986) has demonstrated that the vectors $\boldsymbol{c}_i$ can be found by using the eigenvalue-eigenvector decomposition of the covariance matrix $\boldsymbol{B}$ in the following form:

$$\boldsymbol{B}\boldsymbol{c}_i = \sigma_i^2 \boldsymbol{c}_i \tag{3}$$

and,

$$\boldsymbol{B} = \boldsymbol{A}^{\boldsymbol{T}}\boldsymbol{A} = \frac{1}{M}\sum_{i=1}^{M}\boldsymbol{y}_i\boldsymbol{y}_i^T = \frac{1}{M}\begin{bmatrix} \sum_{i=1}^{M} x_i x_i & \cdots & \sum_{i=1}^{M} x_i x_{i+(m-1)\tau} \\ \vdots & & \vdots \\ \sum_{i=1}^{M} x_{i+(m-1)\tau} x_i & \cdots & \sum_{i=1}^{M} x_{i+(m-1)\tau} x_{i+(m-1)\tau} \end{bmatrix} \tag{4}$$

where σ_i^2 are the eigenvalues of the covariance matrix and the vectors $\boldsymbol{c}_i$ are the associated eigenvectors. The rank of the covariance matrix is equal to the number of its non-zero eigenvalues. The eigenvalues of the covariance matrix form a subspace which dimension is equal to the embedding dimension. Hence it is straightforward to use vectors restricted to this subspace in the pseudo-phase diagrams. The vectors of the trajectory that satisfy this restriction can be calculated multiplying the trajectory matrix by the orthogonal matrix $\boldsymbol{C}$, whose columns are composed by the eigenvectors $\boldsymbol{c}_i$:

$$\boldsymbol{AC} = \begin{bmatrix} \boldsymbol{y}_1^T \\ \boldsymbol{y}_2^T \\ \vdots \\ \boldsymbol{y}_M^T \end{bmatrix}\begin{bmatrix} \boldsymbol{c}_1 & \boldsymbol{c}_2 & \cdots & \boldsymbol{c}_m \end{bmatrix} = \boldsymbol{D} = \begin{bmatrix} \boldsymbol{d}_1 & \boldsymbol{d}_2 & \cdots & \boldsymbol{d}_m \end{bmatrix} \tag{5}$$

The columns of the rectangular matrix $\boldsymbol{D}$ ($\boldsymbol{D} \in \Re^{M\times m}$) plotted in an orthogonal plane form the pseudo-phase portrait. These diagrams are similar to the phase-portrait diagrams once they are constructed using linear transformations of the trajectory matrix. The first problem that arises from the above transformation is the choice of the eigenvectors $\boldsymbol{c}_i$, $i = 1, 2, \cdots, m$, used in the pseudo-phase portrait. For practical machine signals, random or correlated noise is always present, and it is expected that some of the eigenvalues of the covariance matrix to be associated with noise. It is well known that the eigenvalues and eigenvectors are closely related to the natural frequency and mode shape of linear dynamic systems.

The eigenvector complexity is an indicator of the dynamic system complexity. If the noise is random and appears at low intensity, one can use only the two eigenvectors ($\boldsymbol{c}_1$, $\boldsymbol{c}_2$), which are associated to the two biggest eigenvalues of the covariance matrix to form an orthogonal plane defined by the singular vectors ($\boldsymbol{d}_1$, $\boldsymbol{d}_2$). Therefore, only the deterministic part of the trajectory matrix is considered for reconstructing the trajectory and the noise-dominated part is theoretically eliminated. This is an important aspect for practical machine monitoring, because noise is always present in measured signals. However, using only the two largest eigenvalues of the covariance matrix can dissimulate small perturbations of machine operational conditions. Small machine modifications may indicate an incipient fault hence, for monitoring purposes it is important to develop methodologies that are, both, sensible to small variations of machine conditions and also not perturbed by noise.

Another question that arises from the above discussion is the reconstruction of the trajectory matrix. The reconstruction process is based on the determinations of the optimal lag time and the embedding dimension. The use of incorrect lag time or incorrect embedding dimension leads to an inaccurate representation of the true dynamics. There are at least two difficulties in applying the PPP method in real machine monitoring, because the lag time τ and the embedding dimension m must be determined before reconstructing the embedding space. These parameters have large influence on the PPP method and they must be correctly calculated so that the actual state space and its reconstructed form (PPP) are in some sense equivalent. Takens' theorem states the sufficient condition $m \geq 2n+1$ where n is the dimension of the original system. This, however, is of little practical relevance since n is not known a priori. Also, Takens' theorem assumes that infinite amount of noise-free data are available, but it is not the case for practical situations, because the data are always time-limited and corrupted by noise.

Numerical simulations of non-linear systems, have demonstrated that, if τ is too small, the reconstructed attractor falls on the main diagonal of the co-ordinate system and this result in little information gain. On the other side, if τ is too large, successive reconstructed vectors $\boldsymbol{y}_i$ may become uncorrelated and the reconstruction is no longer representative of the true dynamics. This is called irrelevance (Csdagli et al., 1991). It is important to set a lag time to assure that the components of x_i are independent and the same lag time must be used for all embedding dimensions. There are different methods for estimating the lag time such as autocorrelation function and mutual information (Albano et al., 1988, Fraser, 1986). Kugiumtzis (1993), has suggested to set the time window, $(m-1)\tau$, equal to or larger than

the mean orbital period from the oscillations of the time series, which is equal to the mean time between peaks (tbp). This relation states that the embedding dimension and lag time must be defined not separately and it will be investigated further in Section 3.

The influence of embedding dimension *m* is also important in the PPP method. The dimension estimation gives a measure of the necessary and sufficient number of state variables necessary to approximate the steady-state dynamics from which the time series is realized. One approach for determining the embedding dimension is to increase *m* systematically, until the trajectories no longer appear to intersect (Roux et al, 1983). This is a subjective criterion and become inapplicable when the dimension become higher. In the absence of noise, the rank of the trajectory matrix is equal to the number of its non-zero eigenvalues, which form the smallest subspace that represents the trajectory. However, for practical applications, the number of state variables of a real machine is not known a priori. Broomhead (1986) has proposed to define *m* and τ as a function of band-limited frequency and set both not separately in the form: $m \geq (2n+1)\tau = 2\pi / w$, where *w* is the frequency in the Fourier spectrum of time series with the greater power. Using this relation one can estimate the system dimension *n* if the main frequency, *w*, is known. For practical applications, the above relation can be adopted if the main frequency in the FFT spectrum of the time series is clearly visualized. This is the case when one is measuring rotor radial vibrations of a healthy machine, because the synchronous frequency is always present in the FFT spectrum and usually, it has the greater power. Once the dimension *n* is estimated, the embedding dimension can be calculated by using Takens' theorem. However, if the reconstruction process is sufficiently close to the original system map, the embedding dimension can be as small as the system dimension, $m = n$, (Casdagli et al, 1991). Hence, the lowest limit for the embedding dimension could be:

$$m \geq \frac{1}{2}\left(\frac{2\pi}{w\tau} - 1\right) \tag{6}$$

In this paper the embedding dimension and the lag time are calculated by using the above relation. Once the lag time and embedding dimension are defined, the trajectory matrix can be reconstructed directly from the time series. If the reconstruction process is perfect, the most relevant characteristics of the original system are preserved in the reconstructed trajectory and one can use these characteristics for extracting qualitative information from the system. Here, qualitative information means knowledge, which may be obtained from a qualitative analysis of a dynamical system. A practical application of the PPP method for machine condition monitoring will be described on Section 3.

3. Monitoring a vertical rotating machine

In this experiment the orbit diagram, phase-portrait, FFT spectrum and the pseudo-phase portrait method have been employed for condition monitoring of a vertical rotating machine. The vertical test machine used in this experiment is composed by an electric motor with velocity control and a rotor supported by rolling bearings at its upper side and a tilting pad thrust bearing at the lower part of the rotor. A rigid disc is mounted at the end of the shaft and a hydraulic mechanism provides the axial load to the bearing. The vertical test machine and a detailed part are pictured in Fig. (1).

Tilting pad thrust bearings are usual component in large machinery with vertical rotor. However, only recently the influence of an axial bearing on radial vibrations has been reported (Jiang, 1998, 1999). The thrust bearing provides additional stiffness and damping of a flexible shaft, increase the first critical speed and also provides a decrease of the rotor radial vibration. Berger (2000) has investigated the problem of a manufacturing defect in a thrust bearing and he has shown that an angular defect in the stator of the bearing produces a synchronous moment, similar to unbalance response. This result shows that different faults in a practical machine can produce similar characterization in FFT analysis. The thrust bearing used in the vertical machine was considered in perfect conditions for monitoring purposes. By using the hydraulic mechanism it is possible to apply different axial loads to the thrust bearing, and hence, modifying the rotor dynamic behavior. The electric motor provides the rotation to the rotor, which can be controlled using a digital control system.

Two non-contact inductive displacement sensors (Bentley Nevada™ Proximitor 3300 series) were appropriately fixed in X-Y co-ordinate positions to monitor the disc radial vibrations. The Lynx™ digital signal analyzer was utilized for signal acquisition and processing. Matlab™ software routines were elaborated for calculating the orbit diagrams, phase-diagrams and also the FFT spectra. No digital filter was used in all data collected and the sampling frequency was set at 1000 Hz. Then, pseudo-phase portraits were calculated for different rotations and also for different axial loads. Initially the axial thrust bearing used in the vertical rotating machine was considered fault-free and the rolling bearing was also considered in perfect conditions, once all clearances were set to a minimum.

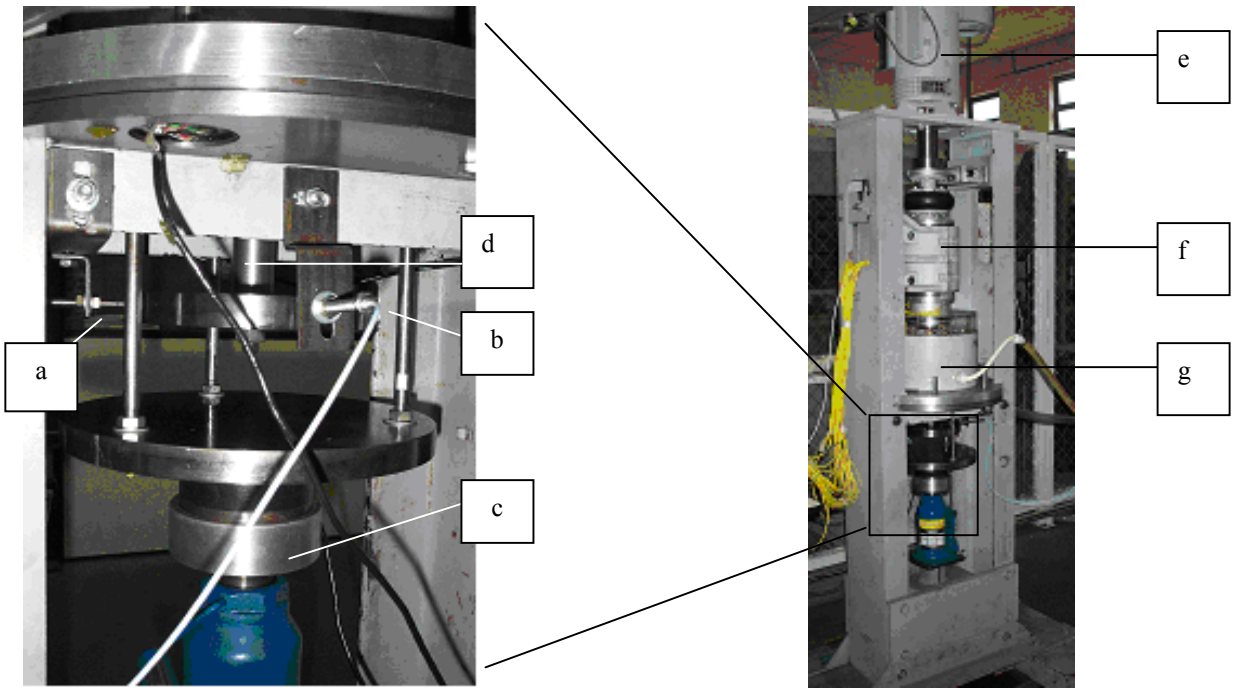

Figure 1. Vertical test machine and a detailed part: a) displacement sensor of X co-ordinate, b) displacement sensor of Y co-ordinate, c) axial load cell and hydraulic mechanism, d) rotor, e) motor, f) rolling bearings, and g) tilting pad thrust bearing.

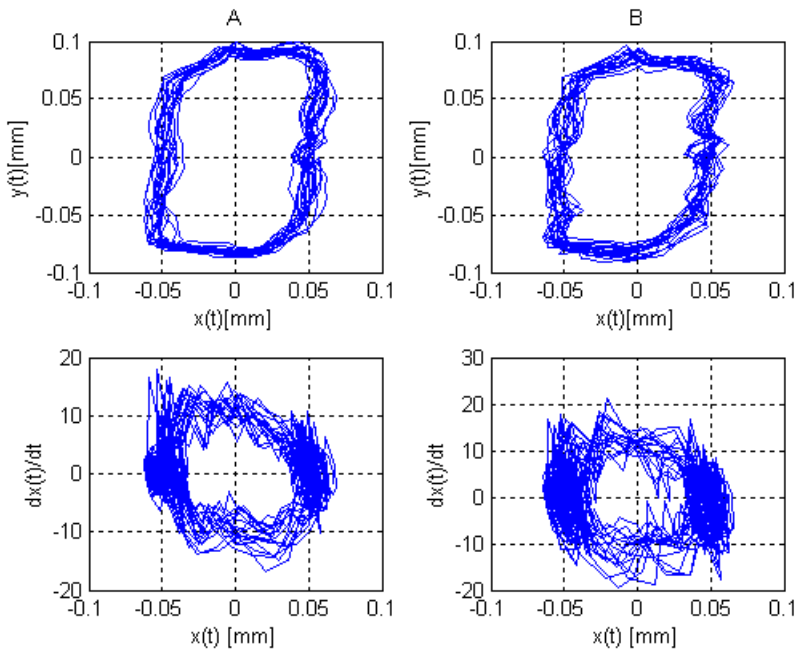

Figure 2. Orbit diagrams calculated from X and Y co-ordinates at 996 r.p.m. and phase portraits calculated from X co-ordinate. The axial load values are: A) 15 kN, B) 20 kN

The orbit diagrams and the phase portraits are presented in Fig. (2). The orbit diagrams show approximately the trajectory of the center of the rotor. It can be verified in these diagrams that the orbits are not perfect circles, because the test machine is not ideal. One could expect to find an increase in the trajectory stability, as an increase in axial load is provided. However, it is difficult to distinguish this effect for such a small variation in axial load. Generally speaking the thrust bearing hinders the deflection of the shaft and hence at the upper limit of axial load, the amplitudes of rotor radial vibrations should be smaller (Jiang, 1999). Observing these trajectories separately one cannot evaluate the health of the entire system. As with any other diagnostic method based in machine symptoms, it is necessary to develop, previously, the patterns of the healthy system to achieve any fault diagnosis.

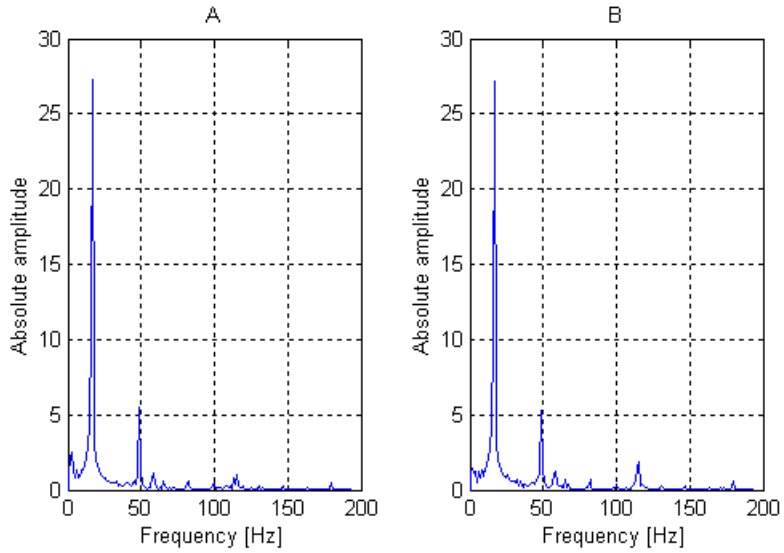

Figure 3. FFT spectra of X co-ordinate at 996 r.p.m. The axial load values are: A) 15 kN, B) 20 kN.

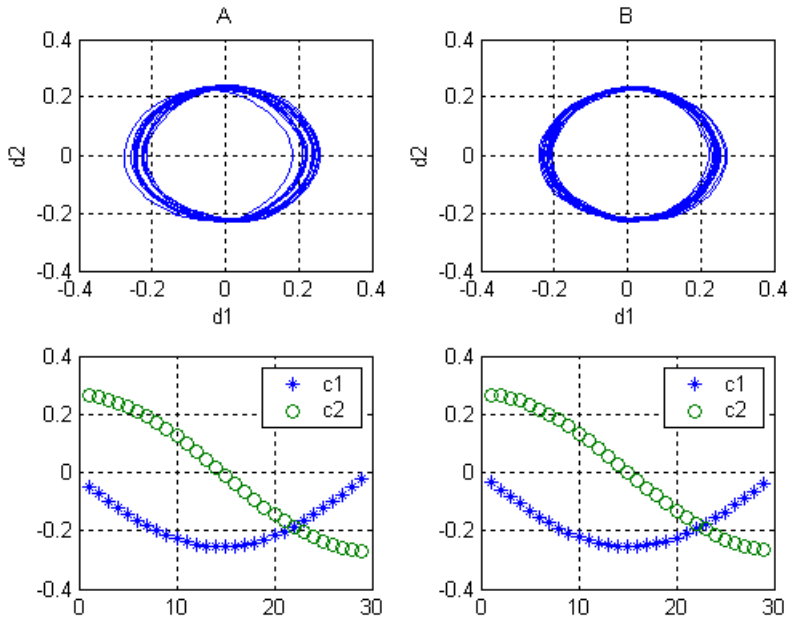

Figure 4. Pseudo-phase portraits and respective eigenvectors c1 and c2, calculated from X co-ordinate at 996 r.p.m. The axial load values are: A) 15 kN, B) 20 kN. Embedding dimension is 29 and lag time is 0.001 s.

The phase portraits of the disc radial displacements were also pictured in Fig. (2) for different axial loads. The phase portraits show a broader pattern than orbit diagrams and it is easy to identify the sharp corners due to the derivatives of raw time series. The axial thrust bearing introduces additional stiffness and damping to the rotor, however, these influence is not clearly observed in the phase portrait diagrams, hence it is difficult to correlate each pattern with its respective axial load. The phase-portrait derive from perfect trajectories probably due to a series of machine imperfection, such as, problems in the manufacturing process of the disc, rotor misalignment, imbalance forces, small ball bearing clearances, etc. However, for monitoring purposes, one could not consider these imperfections and hence, the orbit diagrams and phase portrait could be considered representative of a fault free machine condition.

The FFT spectra for two different axial loads are presented in Fig. (3). An amplitude decrease in the synchronous radial vibration was expected in Fig. (4B) due to the action of the thrust bearing, but this influence is almost imperceptible. When the axial load increase from 16 kN to 20 kN, the main frequency components of the signal show a very small decrease, hence these two different axial loads produce almost the same FFF spectra. Hence, it is difficult to diagnose any machine variation considering the FFT spectra separately. In this case, another auxiliary method should be used to achieve any fault detection and diagnosis.

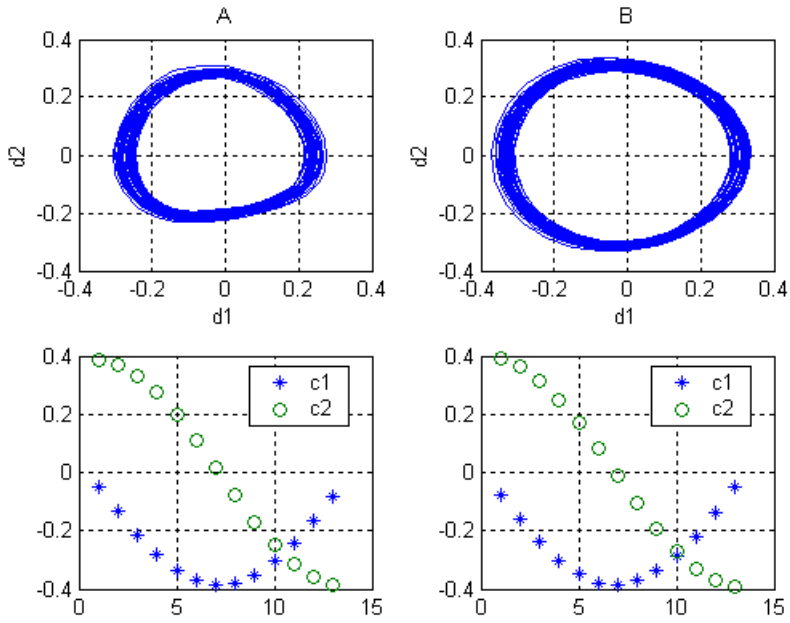

Figure 5. Pseudo-phase portraits and respective eigenvectors c1 and c2 calculated from X co-ordinate at 2226 r.p.m. The axial load values are: A) 15 kN, B) 20 kN. Embedding dimension is 13 and lag time is 0.001 s.

The pseudo-phase portrait for different rotor speeds and axial loads are showed in Fig. (4) and Fig. (5). Observing these diagrams one can verify the presence of more stable attractors, which provide an easier visualization of small variations of machine conditions. The stability properties of PPP can be attributed to the average possess used for computing the singular vectors $\boldsymbol{d}_1$ and $\boldsymbol{d}_2$. The operation of the eigenvectors $\boldsymbol{c}_1$ and $\boldsymbol{c}_2$ in the trajectory matrix results in average values that smoothes the trajectory pattern. The eigenvectors associated to the pseudo-phase diagrams are also pictured in Fig. (4) and Fig. (5). The values of the two biggest eigenvectors of the covariance matrix are almost the same. The biggest eigenvectors are associated to the main frequencies of the signal, and as verified in FFT spectra, the main frequencies variations are almost negligible. Hence, for small variations of axial loads, one can also expect small variations on these eigenvectors.

The presence of noise in the measured signal has great influence in orbit diagrams and phase portrait, but this influence is virtually vanished of PPP computation. This occurs because in the absence of noise, the rank of trajectory matrix, which is equal to the number of its non-zero eigenvalues, is the dimension of the embedding space that contains the trajectory. If the observations are composed by an additive noise in the form: $y(t) = x(t) + r(t)$, where $r(t)$ is a random noise, the noise prevents any eigenvalue from vanishing completely. The first largest eigenvalues of the trajectory matrix mostly arise from the signal and the remaining eigenvalues arrive from the noise. Hence the eigenvalues related to the noise are not used for PPP computation. The computation of PPP using the smallest eigenvectors produces random diagrams that are not representative of the true dynamics.

In Fig. (4) it is possible to visualize the action of the thrust bearing on the system dynamics. The PPP computed in Fig. (4B) is more stable than the PPP computed in Fig. (4A), as expected. In Fig. (5) the PPP was computed using a higher rotation (2226 r.p.m). The thrust bearing provides a better rotor stability at this rotation and its influence on the system dynamic at 15 kN and 20 kN of axial load is virtually the same. However, the PPP differ from each other, allowing the visualization of machine condition variation. From comparison between the phase portraits of Fig. (2) and the pseudo-phase portraits of Fig. (4) one can verify that these diagrams preserve some topological similarities. This is an important characteristic because the main properties of the system dynamics are preserved in pseudo-phase portrait and this facilitates the task of fault detection and diagnostic.

The influence of lag time and embedding dimension on the computation of PPP is now discussed. Equation (6) is used for estimating the embedding dimension, but firstly, it is necessary to calculate the main frequency of the raw time series. The calculation of w is an easy task, once the displacement vectors are recorded on computer and the FFT spectra are available. The X or Y co-ordinates can be used for these calculations. The result is $w = 233$ rd/s, when rotor rotation is 2226 r.p.m. and the sampling frequency is 1 kHz. Adopting the lag time equal to the sampling time ($\tau = 0.001$ s) and using Eq. (6), results in $m \geq 13$. The same method was employed for calculation of the embedding dimension for 996 r.p.m and the results is $m \geq 29$. This method for calculating embedding dimension proved to be a good estimator, once the stability properties of the trajectory was assured.

Figure (6) shows the PPP calculated for two different values of embedding dimensions. In phase space reconstruction theory, the attractor has been found to have more irregular appearance when the embedding dimension is insufficient. This characteristic is confirmed in Fig. (6A), where PPP was calculated with a small embedding dimension.

When the embedding dimension reach the best dimension calculated theoretically ($m = 29$), the patterns become more stable and smooth. In this condition the PPP and phase-portrait preserve some similarities.

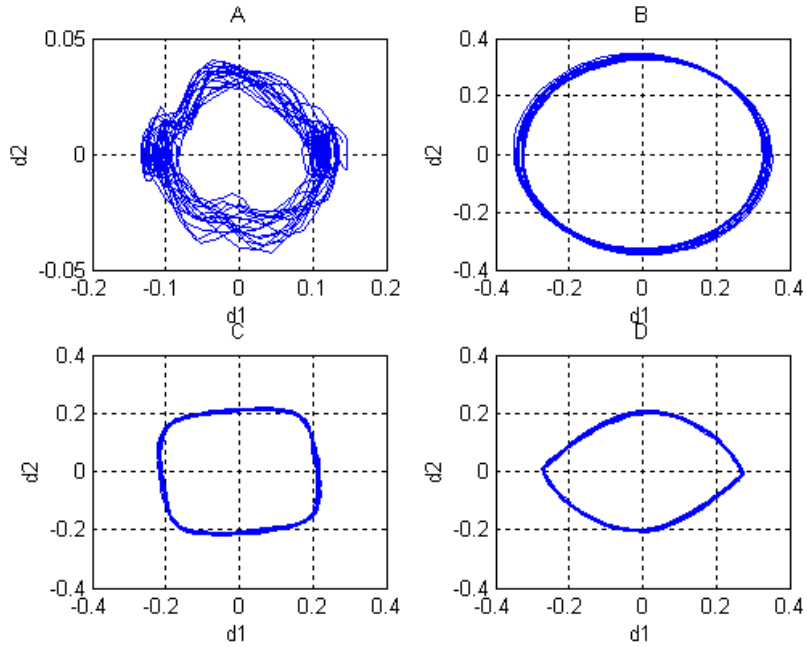

Figure 6. Pseudo-phase portraits calculated for different lag times and embedding dimensions. A) $\tau = 0.001$ s, $m = 5$. B) $\tau = 0.001$ s, $m = 61$. C) $\tau = 0.015$ s, $m = 29$. D) $\tau = 0.030$ s, $m = 29$. The axial load is 20 kN and the rotation is 996 r.p.m. Compare with Fig. (4B).

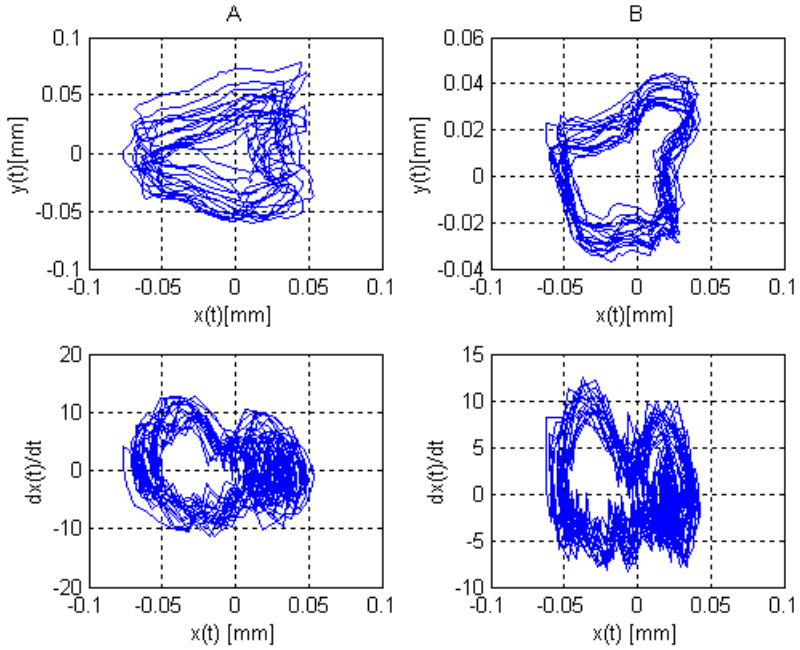

Figure 7. Orbit diagrams calculated from X and Y co-ordinate and phase-portraits calculated from X co-ordinate, with a fault rolling bearing (loose bearing cap) at 996 r.p.m. The axial load values are: A) 2 kN, B) 15 kN.

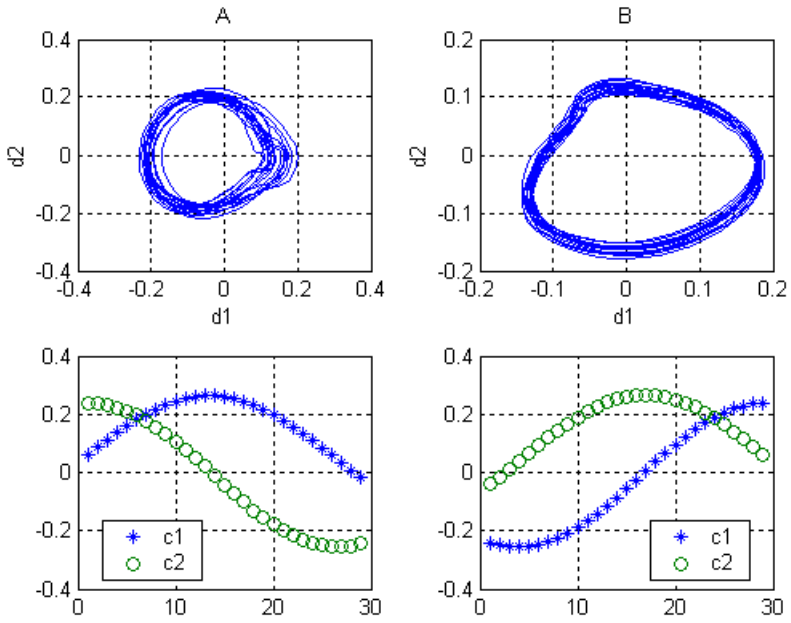

Figure 8. Pseudo-phase portraits and respective eigenvectors c1 and c2, calculated from X co-ordinate, with a fault rolling bearing (loose bearing cap) at 996 r.p.m. The embedding dimension is 29 and lag time is 0.001 s. The axial load values are: A) 2 kN, B) 15 kN. Compare with Fig (7).

By adopting the embedding dimension: $m \geq (tbp/\tau)+1$ as has been suggested in Kugiumtzis' s paper, it results in $m \geq 61$, when the lag time is equal to 0.001 s and the rotational speed is 996 r.p.m. In this case, a larger dimension provides little additional information about the system and the PPP is virtually equal to the PPP calculated using $m = 29$, as shown in Fig. (6B). However, one can choose the smallest embedding dimension possible, for saving computational cost. In practice, it is impossible to decrease the lag time above limit defined by the sampling frequency. Therefore, the small lag time will be limited by limitations imposed by the instrumentation used for collecting raw time series. The best lag time used for PPP calculation was defined by the sampling interval. The computation of pseudo-phase portrait with large lag times, tend to produce non-correlated eigenvectors and the pattern is no longer representative of the true dynamics. These effects can be seen in Fig. (6C) and Fig. (6D).

All calculated diagrams of Figs. (2-6), are patterns of a machine assumed to be fault free. One can now verify the advantage of PPP over conventional methods when some machine fault occurs. A loose bearing cap was artificially introduced in the bearing and the orbit diagrams, phase-portraits and pseudo-phase portraits were calculated. The fault introduces clearances between the rotor and the bearing, and this provides a modification in system dynamics. The dynamic analysis of a rotor with loose pedestal has been reported recently by Goldman (1994) and Muszynka (1995). These papers show that this type of fault introduces strong nonlinear phenomena and in some cases, chaotic motion is observed. The orbit diagrams and phase portrait of Fig. (7) show the trajectory pattern of the rotor with loose bearing caps, for different thrust bearing loads. In this condition, the attractors of the trajectories become more instable, when it is compared to the non-fault case.

The influence of axial load intensity on rotor radial vibrations is visible in the orbit diagrams, because the trajectory becomes less irregular with a large axial load, but this effect is not clear in the phase portrait. Figure (8) shows the pseudo-phase portrait calculated for this fault condition. The PPP diagrams show small discontinuity points and no sharp corners and also, they preserve some similarities with the phase portraits. The action of the thrust bearing is easily visualized in these diagrams, because PPP computed at 15 kN is more regular and stable than PPP computed at 2kN of axial load. Figure (4A) and Fig. (8B) show the PPP computed for the non-fault case and the fault case, respectively, at the same machine rotation and axial load. It is easy to verify the differentiation between the two cases. The extraction and classification of fault indices represent an important issue in the PPP method, as well as, in any other fault diagnosis method based on machine features. These fault indices can be calculated by using, for example, the mean Euclidean distance between the singular vectors of the PPP. The authors are currently working on this subject.

4. Conclusions

In this work, FFT spectra, orbit diagrams and phase portraits have been studied for monitoring small variations in machine conditions. These conventional methods have been compared with the pseudo-phase portrait method by using a vertical test machine supported by rolling bearings and a thrust bearing. It was demonstrated that, it is difficult to evaluate small variations of bearing axial loads observing the FFT spectra, orbit diagrams or phase-portrait separately. The pseudo-phase portrait was compared with the conventional methods and the results showed that PPP are sensitive to

these small variations and its visualization is improved. The pseudo-phase portrait smoothes the trajectories of the conventional phase portrait and also preserves its main properties. The main difficulties in applying the PPP analysis in practical applications are the definitions of the embedding dimension and the lag time, before reconstructing the trajectory matrix. If the embedding dimension is different from the optimum value, the PPP becomes not representative of the true system dynamic. The optimum lag time has been set equal to the sampling interval, which is limited by the instrumentation utilized in the signal processing. A large increase in this value also produces not representative diagrams. A loose bearing cap was also analyzed using the PPP method. The results showed that this fault produces a trajectory pattern that is significantly different from the non-fault case. Therefore, the PPP method proved to be a promising technique for monitoring real machines and also, for detecting machine faults.

5. Acknowledgements

The financial support received for this project from CNPq and FAPEMIG, through grants 460585/2002-2 and TEC 2280/98, is gratefully acknowledged.

6. References

Albano, M. Muench, J. Schwartz, C., 1988, "Singular Value Decomposition and the Grassbergar-Procaccia Algorithm", Physics reviews A, 38, pp. 3107-3026.

Berger, S., Bonneau, O., Frêne, J., 2000, "Influence of Axial Thrust Bearing Defects on the Dynamic Behavior of an Elastic Shaft, Tribology International, 33, pp. 153-160.

Broomhead, D.S., King, G.P., 1986, "Extracting Qualitative Dynamics From Experimental Data", Physics, D29, pp. 217-236.

Casdagli, M., Eubank, S., Farmer, J.D., Gibson, J., 1991, "State Space Reconstruction in Presence of Noise", Physica D, vol. 51, pp. 52-60.

Chen, Y.D., Du, R., 1995, "Fault Features of Large Rotating Machinery and Diagnosis Using Sensor Fusion", Journal of Sound and Vibration, 188(2), pp. 227-242.

Chu, F., Zhang, Z., 1997, "Periodic, Quasi-Periodic and Chaotic Vibrations of a Rub-Impact Rotor System Supported on Oil Film Bearings", International Journal of Engineering Science, 35 (10), pp. 963-973.

Fraser, M., Swinney L., 1986, "Independent Coordinates for Strange Attractors From Mutual Information", Physical Review A, 33, pp. 1134-1140.

Goldman P., Muszynska A., 1994, "Dynamic Effects in Mechanical Structures with Gaps and Impacting: Order and Chaos", Journal of Vibration and Acoustics, 116, pp. 541-457.

Jiang, J.D., Chen, J., 1999, "The Application of Correlation Dimension in Gearbox Condition Monitoring", Journal of Sound and Vibration 223 (4), pp. 529-541.

Jiang, P.L., Yu,L., 1999, "Effect of a Hydrodynamic Thrust Bearing on the Statics and Dynamics of a Rotor-Bearing System", Mechanics Research Communications, Vol.25, 2, pp. 219-224.

Kugiumtzis, D., 1996, "State-Space Reconstruction Parameters in the Analysis of Chaotic Time Series-the Role of the Time Window Length, Physica D 95, pp. 13-28.

Lucifred, A. et al, 2000, "Application of Multiregressive Linear Models, Dynamic Kringing Models and Neural Network Models to Predictive Maintenance of Hydroelectric Power Plants", Mechanical Systems and Signal Processing, 14 (3), pp. 471-494.

Muller, P.C., Bajkowski, J., Soffker, D., 1994, "Chaotic Motions and Fault Detection in a Cracked Rotor", Nonlinear Dynamics 5, pp. 233-254.

Muszynska, A, Goodman, P., 1995, "Chaotic Responses of Unbalanced Rotor/Bearing/Stator Systems with Looseness or Rubs", Chaos, Solutions and Fractals, 5, pp. 1683-1704.

Roux, J.C., Simoy, R. H., Swinney, H.L., 1983, "Observation of a Strange Attractor", Physica D 8, pp. 257-266.

Takens, F., 1981, "In Lecture Notes in Mathematics", Berlin: Springer D. A. Rand and L.S. Yong (eds). Detecting strange attractors in turbulence, pp.366-342.

Wang, W.J. Chen, J., 2001, "The Application of Some Non-Linear Methods in Rotating Machinery Fault Diagnosis", Mechanical Systems and Signal Processing, 15 (4), pp. 697-705.

Wang, W.J., Lin, R.M., 2003, "The Application of Pseudo-Phase Portrait in Machine Condition Monitoring", Journal of Sound and Vibration, 259 (1), pp.1-16.

Wang, W., Chen, J., Wu, Z., 2000, "The Application of a Correlation Dimension in Large Rotating Machinery Fault Diagnosis", Proc. Instn. Mech. Engrs., vol. 214, part C, pp. 921-930.